Offprint from

Proceedings of the

Seventh European Conference on Mathematics in Industry

March 2–6, 1993 Montecatini Terme

Edited by

Antonio Fasano
Mario Primicerio

Universita di Firenze
Dipartimento Di Matematica "U. Dini"

B. G. Teubner Stuttgart

Resonant responses and chaos in nonlinear drillstring dynamics[1]

G.H.M. van der Heijden

Mathematics Institute, University of Utrecht
Utrecht, The Netherlands

1 The model

We investigate a model proposed to describe the lateral vibrations of a rotating stabilised drillstring as is used in drilling oil wells. A schematic picture of the underground part of a drilling assembly is given in Fig. 1. Usually it consists of a rock-crushing tool (the bit) at the lower end of a series of tubular sections (collars) supported by regularly spaced stabilisers. A small play between stabiliser and wall (inevitable in practice) introduces a nonlinearity in our model which will turn out to give rise to complicated dynamical behaviour.

In deriving the equations of motion we assume that the hole is in the vertical and that the deflected shaft is in its first bending mode so that we have a two-degrees-of-freedom system (this is justified by the relatively low rotary speeds, often close to the natural bending frequency of the shaft, in actual drilling). Also, the stabilisers are considered massless. Then the equations of motion of an isolated section of the drillstring between two stabilisers can be written, in terms of the complex variable $y = y_1 + iy_2$, as follows:

$$\ddot{y} + \gamma\dot{y} + \alpha(1 - \frac{\delta}{|y|})y = \varepsilon\omega^2 \exp i\omega t, \tag{1}$$

where

$$\alpha = \begin{cases} 0 & \text{if } r = |y| = \sqrt{{y_1}^2 + {y_2}^2} \leq \delta \\ 1 & \text{if } r = |y| = \sqrt{{y_1}^2 + {y_2}^2} > \delta. \end{cases}$$

The equation has already been scaled into nondimensional form using the maximum possible deflection $\frac{1}{2}(D_h - D_c)$ (D_h and D_c being the hole and collar diameter respectively, see Fig. 1) and the natural bending frequency of the section as reference length and frequency, respectively.

[1]This work was supported by Shell Research B.V.

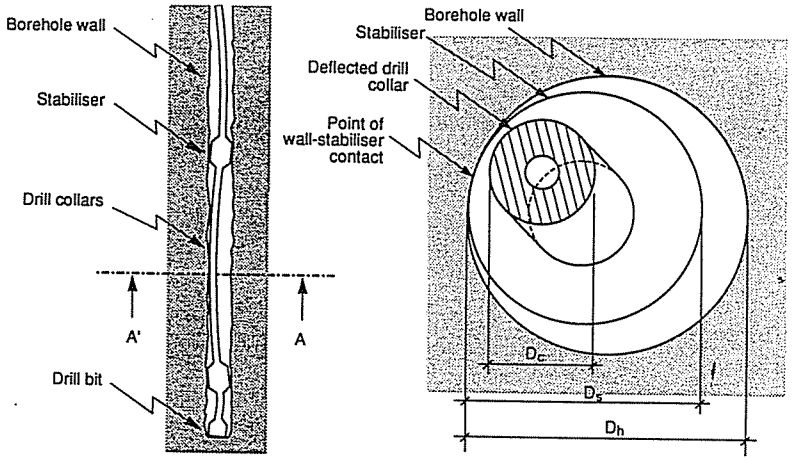

Fig. 1: Deflected drill collar section (left). Section A-A' through the borehole and the deflected drill collar (right).

In equation (1) the co-ordinates y_1 and y_2 represent two orthogonal displacements of the geometric centre of the drill collar relative to the centre of the hole, in a plane perpendicular to the borehole axis half way between the two stabilisers (see Fig. 1). γ is a linear damping coefficient, ω is the driving frequency, ε the mass eccentricity of the collar and δ is the stabiliser clearance. α expresses the fact that, because the stabilisers are taken massless, an elastic restoring force will only act when the radial deflection r exceeds the stabiliser-wall clearance δ, i.e. when the stabiliser is in contact with the wall. This force, then, is proportional to the displacement of the deflected collar with respect to the stabiliser centre.

The immediate observation that the equation of motion (1) becomes autonomous (time-independent) in a co-ordinate system $x = x_1 + ix_2$ rotating with the frequency of forcing ω, i.e. $x = y\exp(-i\omega t)$, will be useful in discussing the dynamics of the model in the following sections. To end this section we refer to [1,2] for more details on modelling drillstring dynamics, and to [3-5] for related models in nonlinear rotordynamics.

2 Synchronous forward whirl

The simplest solutions of (1) are the so-called synchronous forward whirl solutions. The drill collar then performs a circular motion around the centre of the hole with frequency equal to the frequency of forcing ω. Obviously, these solutions can be obtained as fixed point solutions of the system in co-rotating

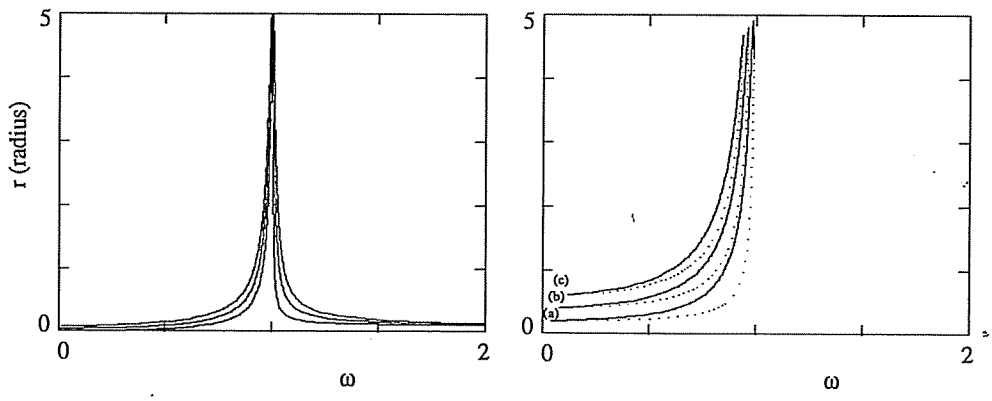

Fig. 2: Forward whirl curves ($\varepsilon = 0.1$, $\gamma = 0.02$). Clearances less than ε_0: $\delta = 0, 0.04$, 0.08 (curves slightly shift to the right for increasing δ) (left); clearances larger than ε_0: $\delta = 0.2$ (a), 0.4 (b), 0.6 (c) (right). Solid lines represent stable, dotted lines unstable solutions.

co-ordinates. For zero clearance, $\delta = 0$, there is, for all ω, a unique forward whirl solution, which also acts as a global attractor. For non-zero δ there turn out to be two cases, depending on the size of the clearance δ relative to the size of the mass eccentricity ε. More precisely, the limiting case is not exactly $\delta = \varepsilon$ but rather $\delta = \varepsilon_0$ where $\varepsilon_0 = \varepsilon\sqrt{1 - \gamma^2 + \mathcal{O}(\gamma^4)}$. In Fig. 2 frequency-response curves are given for both cases. For $\delta < \varepsilon_0$ there is stable whirl for all rotary speeds ω higher than a certain value (which is very small). In contrast, for $\delta > \varepsilon_0$ whirl is only possible for rotary speeds up to a certain speed (which is less than 1). For more details on the exact nature of this distinction (in terms of the bifurcations involved) we refer to [1]. For the present purpose it is important to note that no whirl is possible for $\delta > \varepsilon_0$ and $\omega > 1$, so the question, to be answered in the next section, is: what kind of motion occurs in this region of parameter space.

3 Quasi-periodic solutions and chaos

In the region of parameter space where no simple whirl is possible ($\delta > \varepsilon_0$, $\omega > 1$) we find, in co-rotating co-ordinates, a whole family of seemingly related limit cycles. Examples are shown in Fig. 3. They may be characterised by the number of loops they develop in the (x_1, x_2)-plane. We will call them n-loops, n referring to this number of loops. Solutions with up to 10 loops have been observed. Note that these solutions correspond to quasi-periodic motions of the drill collar in fixed co-ordinates.

Continuing some of the n-loops we obtain Fig. 4, showing the wedge-shaped

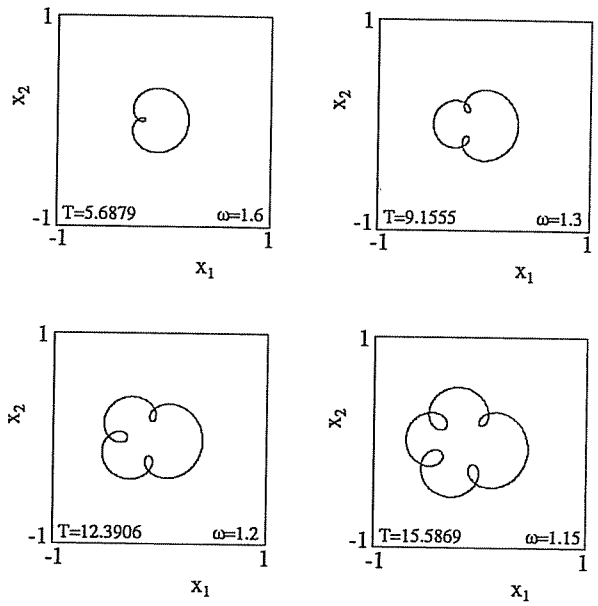

Fig. 3: n-loops in co-rotating co-ordinates ($\delta=0.2$, $\varepsilon=0.1$, $\gamma=0.01$). T denotes the period.

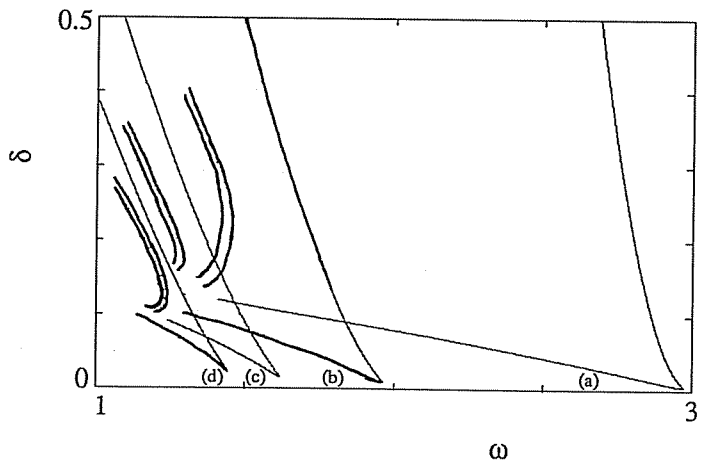

Fig. 4: Resonance tongues for the 1-loop (a), 2-loop (b), 3-loop (c) and 4-loop (d). Also drawn are some first and second period-doubling curves ($\varepsilon=0.1$, $\gamma=0.01$).

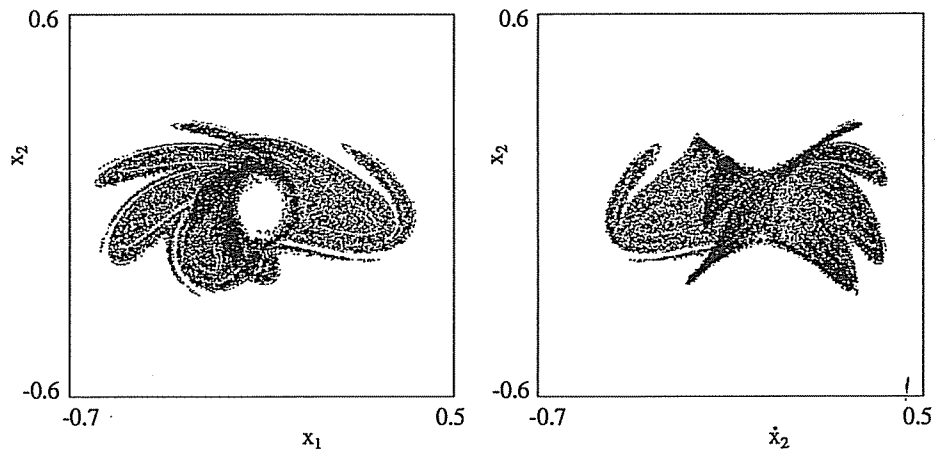

Fig. 5: Projections of a Poincaré section of the chaotic attractor for $\omega = 1.12$, $\delta = 0.2$, $\varepsilon = 0.1$ and $\gamma = 0.01$.

regions (also called tongues) of their existence in the (ω, δ)-plane. On the boundaries of these tongues saddle-node bifurcations occur in which the n-loops annihilate with their unstable partners (the resonance curves are closed curves). In between the tongues motion eventually reaches the fixed point solutions for $\delta < \varepsilon_0$ discussed in the previous section (these solutions, by the way, also exist, along with the n-loops, for parameters inside the tongues, as long as $\delta < \varepsilon_0$)

For decreasing damping γ the tongues become wider and move down towards the ω-axis. Indeed, in the limit of zero damping they seem to touch the frequency axis at simple rational values of ω. For instance, for the 1-, 2- and 4-loop these base frequencies would appear to be 3, 2 and $\frac{3}{2}$, respectively.

For low values of δ the tongues are disjoint, but for $\delta \approx 1$ they start to overlap. Two or more different n-loops then coexist for the corresponding parameters. In the regions of overlap the n-loops each individually undergo a series of period-doubling bifurcations for decreasing ω. In Fig. 4 first and second period-doubling curves for the 1-, 2- and 3-loop have been included. After these period-doubling cascades chaotic motion is found. For the 3-loop chaotic attractor two projections of the (3-dimensional) Poincaré section (with the plane $\dot{x}_1 = 0$) are shown in Fig. 5. They clearly feature the structure of folded and nested lines typical of chaotic attractors. Quantitative evidence for chaotic behaviour comes from a calculation of the Lyapunov exponents (yielding $\lambda_1 = 0.176$, $\lambda_2 = 0$, $\lambda_3 = -0.0145$, $\lambda_4 = -0.191$), confirming the occurrence of a positive Lyapunov exponent, which is often taken as the definition of chaotic dynamics.

The situation sketched above, in particular the behaviour of the tongues, is

strongly suggestive of a resonance nature of the n-loops (compare, for instance, [6,7]), as indeed will be established in the next section.

4 Resonances

To gain more insight into the origin of the n-loops it is useful to return to fixed co-ordinates. For $\delta = \gamma = 0$ system (1) reduces to a linear system whose solutions can be written down immediately. They contain two frequencies, the scaled natural frequency and the driving frequency ω, and are periodic for rational and quasi-periodic for irrational ω. Since our n-loop tongues emerge from rational ω on the frequency axis in the (ω, δ)-plane, it would appear that for nonzero δ some of these periodic solutions of the linear model are entrained by the nonlinearity. Recall however that the n-loops correspond to quasi-periodic solutions in fixed co-ordinates. So, where does the additional frequency come from?

To answer this question note that the linear system obtained from (1) by putting $\delta = \gamma = 0$ has a twofold natural frequency 1, as dictated, of course, by the symmetry of the problem. Now, it turns out that the nonlinearity resolves this degeneracy, creating two distinct frequencies out of the one natural frequency of the linear model.

Having established the existence of three frequencies for finite δ (two internal frequencies and the forcing frequency), one could anticipate approximate solutions in the form of a sum of the corresponding harmonics:

$$\begin{aligned} y_1(t) &= a_{11}\cos(\omega_1 t + \varphi_{11}) + a_{12}\cos(\omega_2 t + \varphi_{12}) + a_{13}\cos(\omega t + \varphi_{13}) \\ y_2(t) &= a_{21}\cos(\omega_1 t + \varphi_{21}) + a_{22}\cos(\omega_2 t + \varphi_{22}) + a_{23}\cos(\omega t + \varphi_{23}), \end{aligned} \tag{2}$$

where ω_1 and ω_2 are the two internal frequencies and ω is the driving frequency. It is well-known, however, that, in coupled oscillators, a response of this form is only possible if the frequencies are commensurate, i.e. if they satisfy a resonance condition like

$$n_1\omega_1 + n_2\omega_2 = n\omega, \tag{3}$$

for certain integers n_1, n_2 and n. The physical reasoning, of course, is that only a forcing appropriately tuned to the internal cycles is able to effectively supply energy to the system to compensate for the energy loss due to damping.

To verify whether conditions of the form (3) hold for our quasi-periodic solutions we numerically computed their power spectra. The spectra of all quasi-periodic solutions corresponding to n-loops in co-rotating co-ordinates were found to be composed of frequencies $n_1\bar{\omega}_1 + n_2\bar{\omega}_2$ with $\bar{\omega}_1$ and $\bar{\omega}_2$ the

two major frequencies and n_1, n_2 non-negative integers satisfying $|n_2 - n_1| = 1$. What's more, the speculated resonances are indeed found: for each solution a specific linear combination of $\bar{\omega}_1$ and $\bar{\omega}_2$ in its spectrum locks onto the forcing frequency,i.e. $n_1\bar{\omega}_1 + n_2\bar{\omega}_2 = \omega$ for certain n_1, n_2, which depend on the particular n-loop considered. Results for the first ten n-loops are listed in Table 1.

n-loop	resonance
1-loop	$2\bar{\omega}_1 + \bar{\omega}_2 = \omega$
2-loop	$\bar{\omega}_1 + 2\bar{\omega}_2 = \omega$
3-loop	$3\bar{\omega}_1 + 2\bar{\omega}_2 = \omega$
4-loop	$2\bar{\omega}_1 + 3\bar{\omega}_2 = \omega$
5-loop	$4\bar{\omega}_1 + 3\bar{\omega}_2 = \omega$
6-loop	$3\bar{\omega}_1 + 4\bar{\omega}_2 = \omega$
7-loop	$5\bar{\omega}_1 + 4\bar{\omega}_2 = \omega$
8-loop	$4\bar{\omega}_1 + 5\bar{\omega}_2 = \omega$
9-loop	$6\bar{\omega}_1 + 5\bar{\omega}_2 = \omega$
10-loop	$5\bar{\omega}_1 + 6\bar{\omega}_2 = \omega$

Table 1

n-loop	resonance	ω_0
1-loop	$2\omega_1 + \omega_2 = \omega$	3
2-loop	$3\omega_1 + \omega_2 = 2\omega$	2
3-loop	$3\omega_1 + 2\omega_2 = 3\omega$	$\frac{5}{3}$
4-loop	$2\omega_1 + \omega_2 = 2\omega$	$\frac{3}{2}$
5-loop	$4\omega_1 + 3\omega_2 = 5\omega$	$\frac{7}{5}$
6-loop	$5\omega_1 + 3\omega_2 = 6\omega$	$\frac{4}{3}$!
7-loop	$5\omega_1 + 4\omega_2 = 7\omega$	$\frac{9}{7}$
8-loop	$3\omega_1 + 2\omega_2 = 4\omega$	$\frac{5}{4}$
9-loop	$6\omega_1 + 5\omega_2 = 9\omega$	$\frac{11}{9}$
10-loop	$7\omega_1 + 5\omega_2 = 10\omega$	$\frac{6}{5}$

Table 2

A thorough inspection of the spectral analysis results reveals that the major frequencies $\bar{\omega}_1$ and $\bar{\omega}_2$ are not just the perturbed natural frequencies which split from the degenerate frequency of the linear model. In fact, they have a different interpretation depending on whether n is even or odd. Explicitly, the measured frequencies $\bar{\omega}_1$ and $\bar{\omega}_2$ can be identified in terms of the ω_1 and ω_2 (with the behaviour: $\omega_1, \omega_2 \to 1$ if $\delta, \gamma \to 0$) as follows:

$$\bar{\omega}_1 = \frac{\omega_1}{n}, \qquad \bar{\omega}_2 = \frac{\omega_2}{n} \qquad \text{for an odd } n\text{-loop}$$

(4)

$$\bar{\omega}_1 = \frac{\frac{1}{2}(\omega_2 - \omega_1)}{\frac{1}{2}n}, \quad \bar{\omega}_2 = \frac{\omega_1}{\frac{1}{2}n} \qquad \text{for an even } n\text{-loop.}$$

Remark that, apparently, (2) is only valid for $\bar{\omega}_1$ and $\bar{\omega}_2$ in place of ω_1 and ω_2.

Using Table 1 and the relations in (4) we can now derive the resonance relations for the n-loops in terms of the ω_1 and ω_2. Results are given in Table 2, from which the trend for increasing n is transparent. We have also listed ω_0 which is defined as the base frequency from which the resonance tongues emerge and which can now easily be found by putting $\omega_1 = \omega_2 = 1$. In fact, it is readily checked that for an arbitrary n-loop ω_0 is given by the simple formula

$$\omega_0 = 1 + \frac{2}{n}, \tag{5}$$

consistent with results in Fig. 4 as well as with more extensive numerical calculations. Formula (5) suggests that solutions with more and more loops exist

for increasingly narrower resonance tongues which accumulate to the principal resonance of the system located at $\omega = 1$. More results will be published elsewhere.

5 Discussion

We have studied a simple model for drillstring dynamics. The nonlinearity introduced by stabiliser-wall clearance turns out to induce a whole series of quasi-periodic responses which can be traced to entrainments of periodic solutions of the associated linear problem.

For parameter values well within the region of practical significance chaotic motion is found which seems to be associated with overlapping resonances.

As to the practical implications of the various types of motion we note that for the present scaling $r = 1$ means that the drill collar hits the wall. Our results show that for the quasi-periodic and chaotic responses, in general, collar-wall contact will not occur. The forward whirl, however, may cause unwanted drill collar rub against the wall if ω is close to 1.

Another threat to the proper operation of the drilling assembly is presented by fatigue (especially in the threaded connections between sections) caused by strongly fluctuating bending moments. Forward whirl, representing just a rigid rotation of the shaft around the borehole axis, yields constant bending moments. The other types of motion, however, most notably the chaotic motion, may cause bending moments to vary considerably.

References

[1] G.H.M. van der Heijden, *Chaos, Solitons & Fractals* 3, 219-247 (1993).

[2] J.D. Jansen, *J. of Sound and Vibration* 147, 115-135 (1991).

[3] Y.B. Kim, S.T. Noah, *Nonlinear Dynamics* 1, 221-241 (1990).

[4] W.B. Day, *Quart. Appl. Math.* 44, 779-792 (1987).

[5] F.F. Ehrich, *J. of Vibration and Acoustics* 113, 50-57 (1991).

[6] D.G. Aronson, R.P. Mc Gehee, I.G. Kevrekidis, R. Aris, *Phys. Rev.* A33, 2190-2192 (1986).

[7] M.H. Jensen, P. Bak, T. Bohr, *Phys. Rev.* A30, 1960-1969, (1984), *Phys. Rev.* A30, 1970-1981 (1984).